nature methods

Supplementary information

https://doi.org/10.1038/s41592-025-02713-3

SpotSweeper: spatially aware quality control for spatial transcriptomics

In the format provided by the authors and unedited

Table of Content

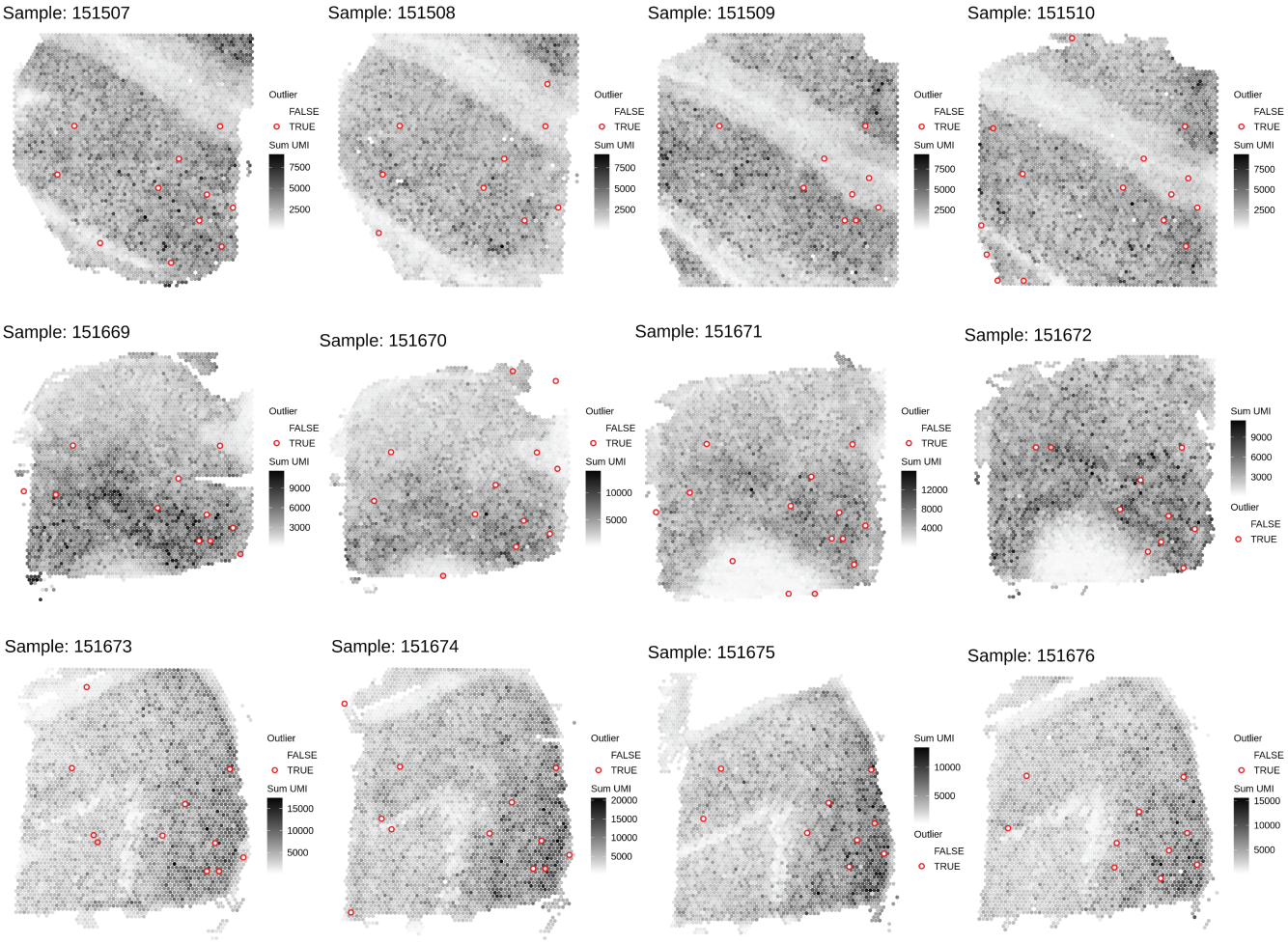

Supplementary Figure S1: Visualization of local outliers across all DLPFC Visium samples (n=12) from Maynard et al [9]. Each plot displays the total UMI counts (library size) across spots in gray scale with local outliers visualized with a red border. Local outliers shown here are any spot that was an outlier in either library size, detected genes, or mitochondrial percentage metrics. Spots at 6 spatial coordinates are consistently identified as low quality across all samples.

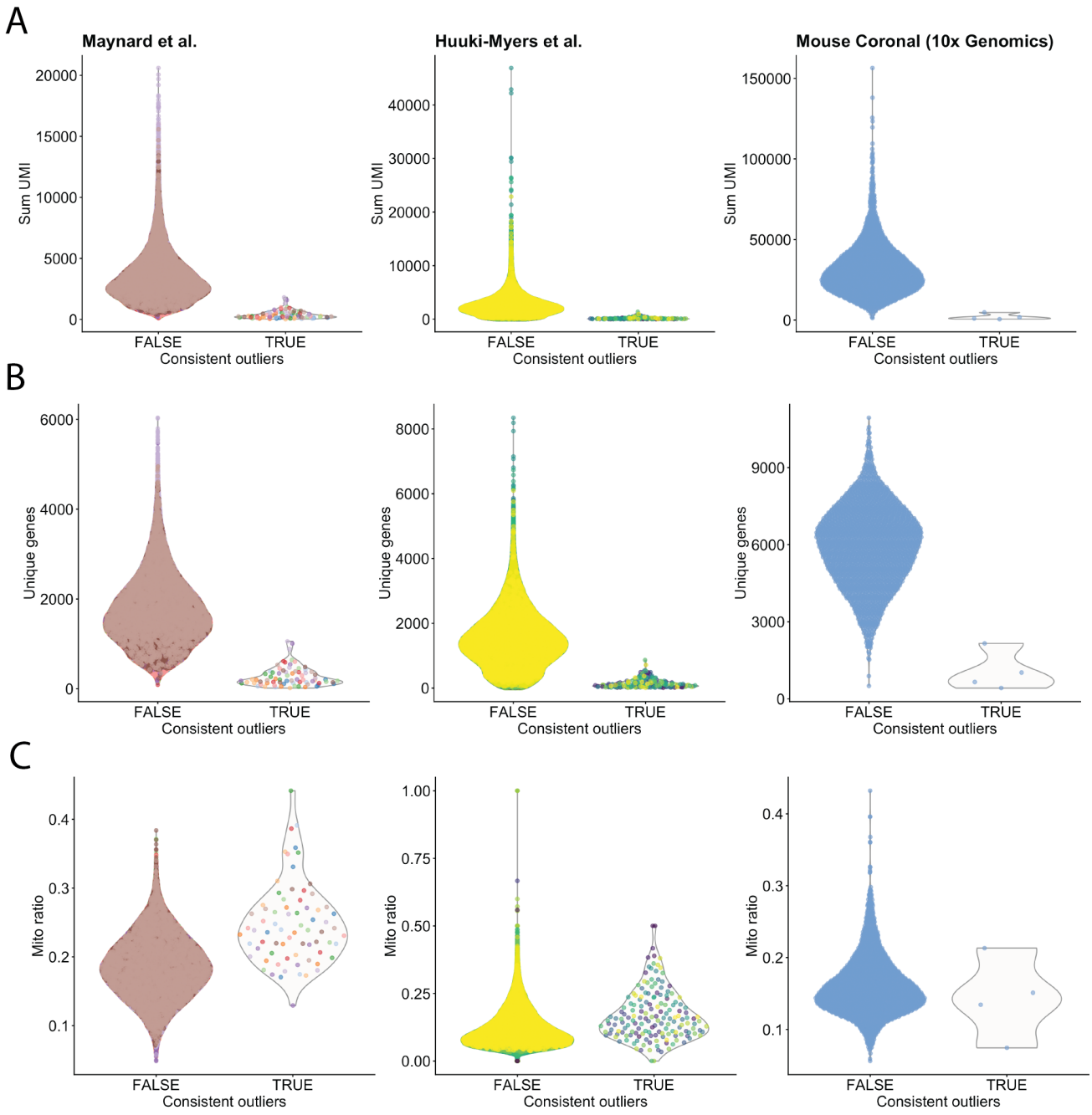

Supplementary Figure S2: Standard QC metrics in the systematic local outliers Violin plots showing standard QC metrics library size (A), unique genes (B), and mitochondrial ratio (C) for the six spots that are consistent outliers across Maynard et al. (n=12), Huuki-Myers et al. (n=30), and mouse coronal section datasets (n=1). All plots are color by sample. Only spots underlying tissue samples were included.

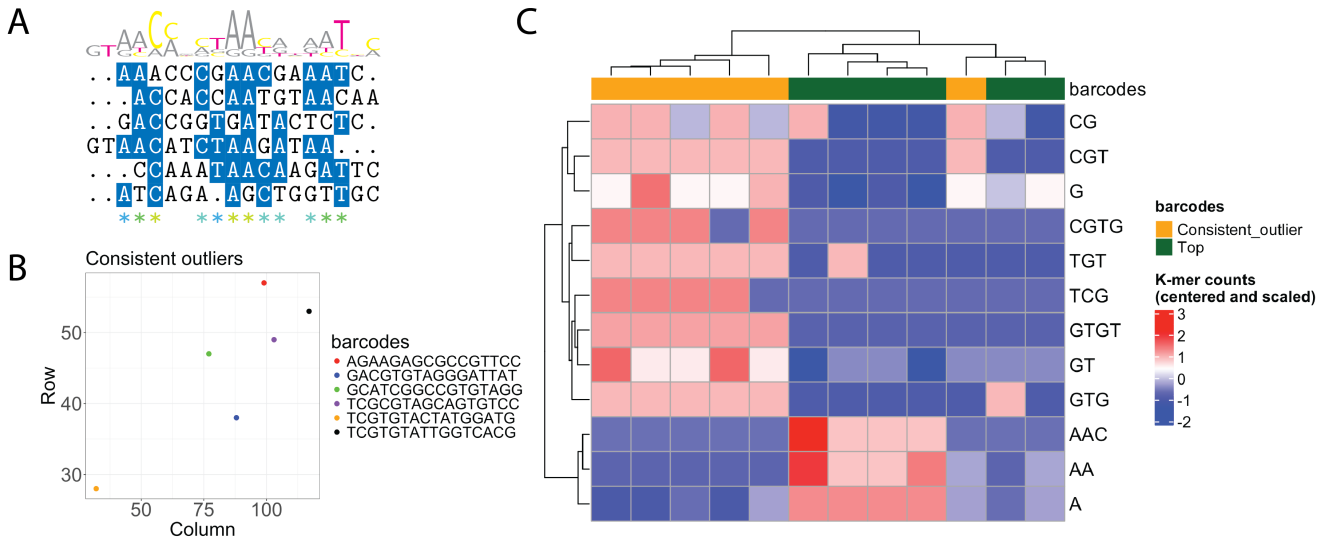

Supplementary Figure S3: Descriptive analysis characterizing the systematic local outlying Visium barcodes and the top mean-ranked barcodes. (A) Sequence alignment of the top six mean-ranked barcodes reveals relatively little homology across barcodes. (B) The barcodes of the six consistent outlier Visium spots and their spatial coordinates. (C) Heatmap of centered and scaled counts for differentially expressed ($p < 0.05$) k-mers between consistent outliers and the top six mean-ranked barcodes. Hierarchical clustering of the columns and rows nearly perfectly distinguished outliers from top ranked barcodes, demonstrating substantial homology within the groups.

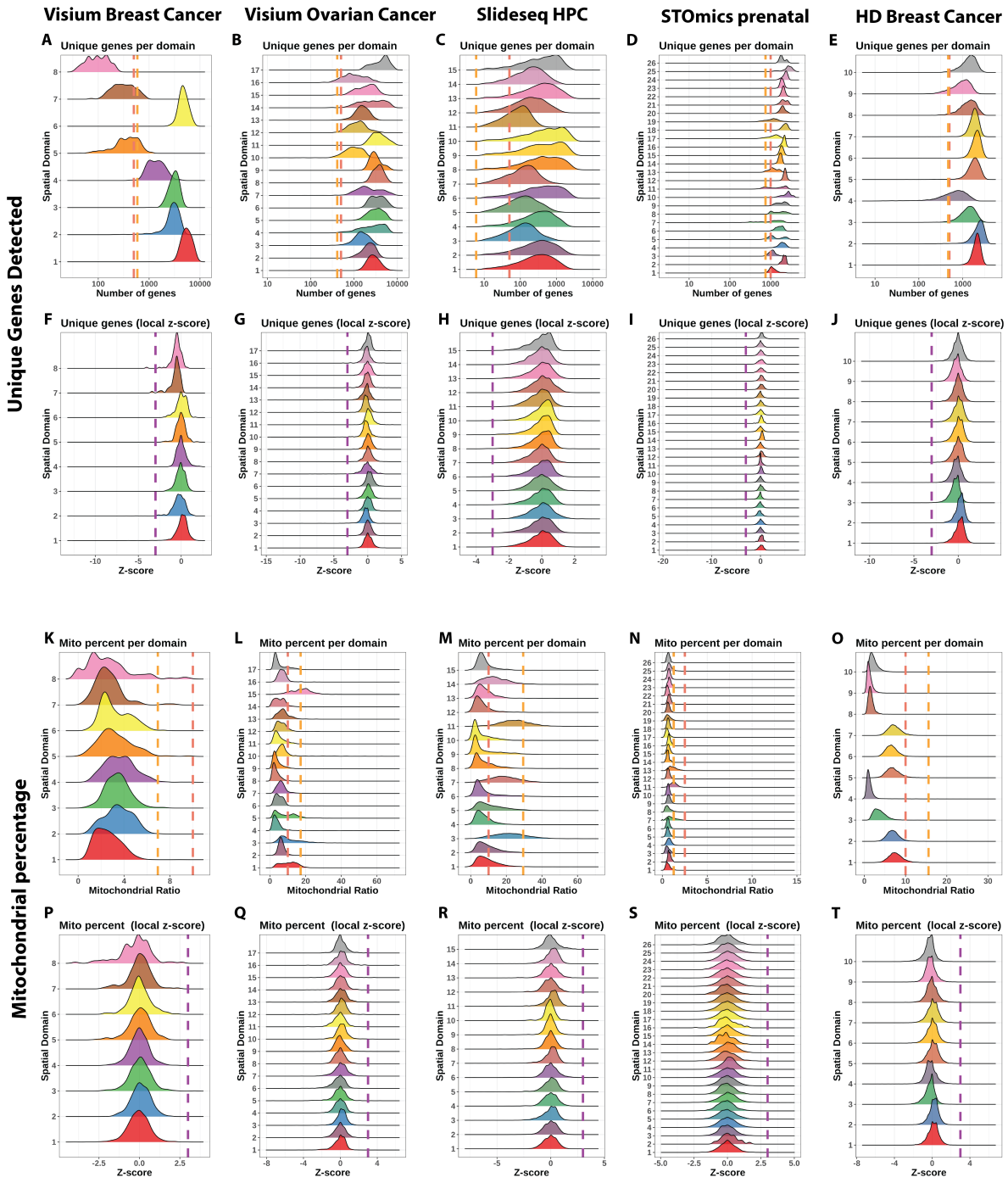

Supplementary Figure S4: SpotSweeper addresses spatial confounding in the unique genes detected and mitochondrial percentage across tissue types and sequencing-based technologies. (**A-E**) Ridge plots of the unique genes detected demonstrates substantial spatial confounding across spatial domains in Visium human breast cancer (**A**), Visium human ovarian cancer (**B**), Slide-seq mouse hippocampus (**C**),Stereo-seq mouse embryonic tissue (**D**), and VisiumHD human breast cancer datasets (**E**). Yellow and orange lines represent data driven (MAD) and fixed QC thresholds, respectively. (**F-J**) SpotSweeper's local outlier detection successfully reduces QC bias across each tissue and technology by normalizing QC metrics, such as library size shown. Purple dashed line represents a fixed threshold of z-score < -3. (**K-T**) Ridge plots showing bias in mitochondrial percentage across spatial domains for each dataset (**K-O**) is also successfully accounted for by SpotSweeper (**P-T**)

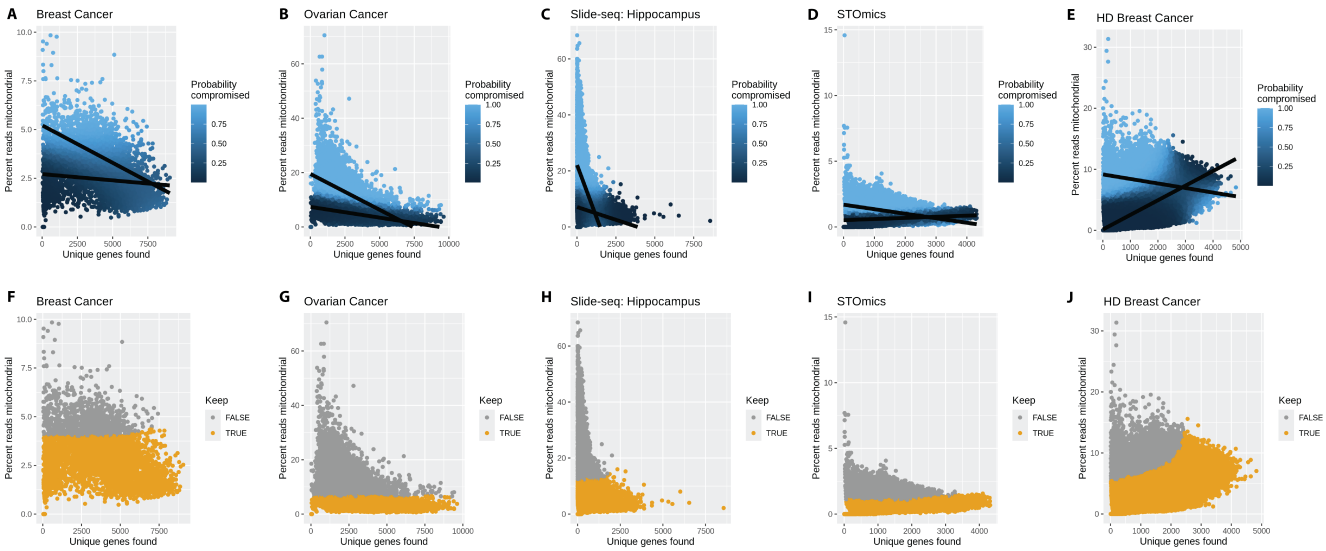

Supplementary Figure S5: Outlier detection performance with miQC which joint models the unique genes detected and mitochondrial percentage. Scatter plots of unique genes detected versus mitochondrial percentage for Visium human breast cancer (**A&F**), Visium human ovarian cancer (**B&G**), Slide-seq mouse hippocampus (**C&H**),Stereo-seq mouse embryonic tissue (**D&I**), and VisiumHD human breast cancer datasets (**E&J**). The top row (**A-E**) displays the best fit linear models (black lines) with the probability with data points colored by the probability of being compromised, defined by high mitochondrial percent and low library size. The bottom row (**A-E**) shows the spots flagged as low quality and discarded (FALSE; gray) versus those that were kept (TRUE; orange).

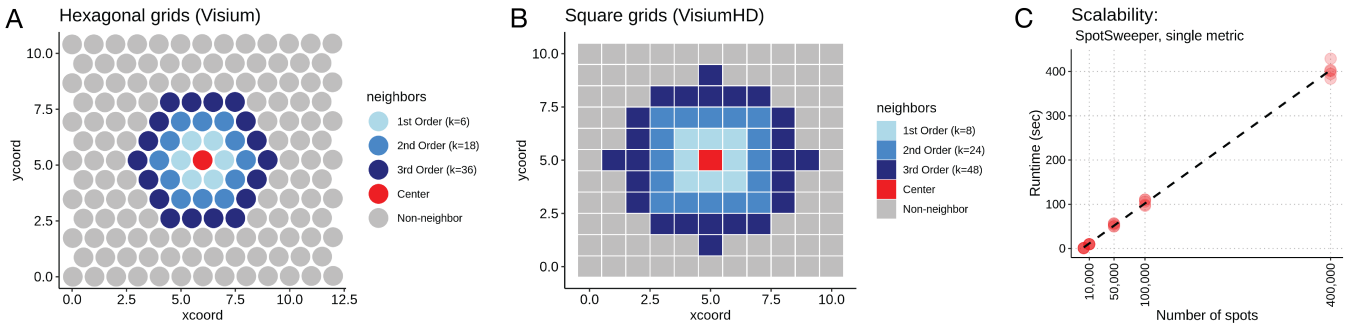

Supplementary Figure S6: Parameter selection and scalability. Number of k nearest neighbors to achieve 1^{st} to 3^{rd} order neighbors in (**A**) hexagonal grids (e.g., Visium), and (**B**) square grids (e.g., VisiumHD and Stereo-seq). (**C**) SpotSweeper's `localOutlier` function scales linearly with the number of spots, taking approximately 1 second per 1,000 spots per metric when ran on a VisiumHD dataset with 3^{rd} order neighbors (k=48) on a single CPU.

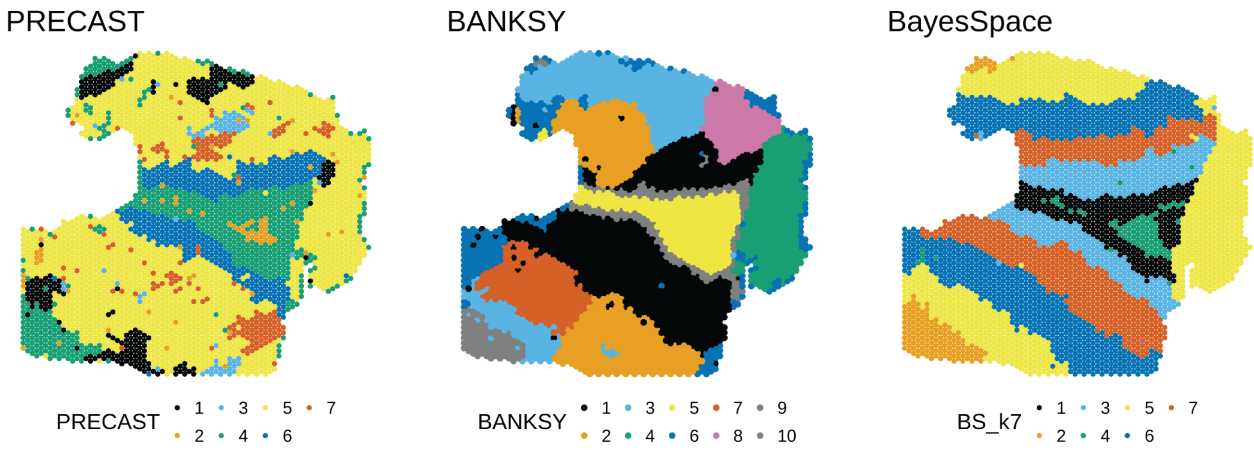

Supplementary Figure S7: Spatial clustering algorithms fail to identify the hangnail artifact as a stand-alone cluster. Spatial clustering results with three algorithms, including PRECAST (left), BANKSY (center), and BayesSpace (right), applied to the Visium DLPFC dataset with the hangnail artifact. While all methods capture some spatial patterns in the data, none successfully identify the hangnail artifact and correctly outline the cortical structure. While BANKSY's cluster 4 (green) does identify most of the hangnail, it fails to include many edge spots and cannot automatically annotate the hangnail, unlike SpotSweeper. This highlights limitations in the sensitivity of these algorithms for detecting regional artifacts in spatial transcriptomics data.

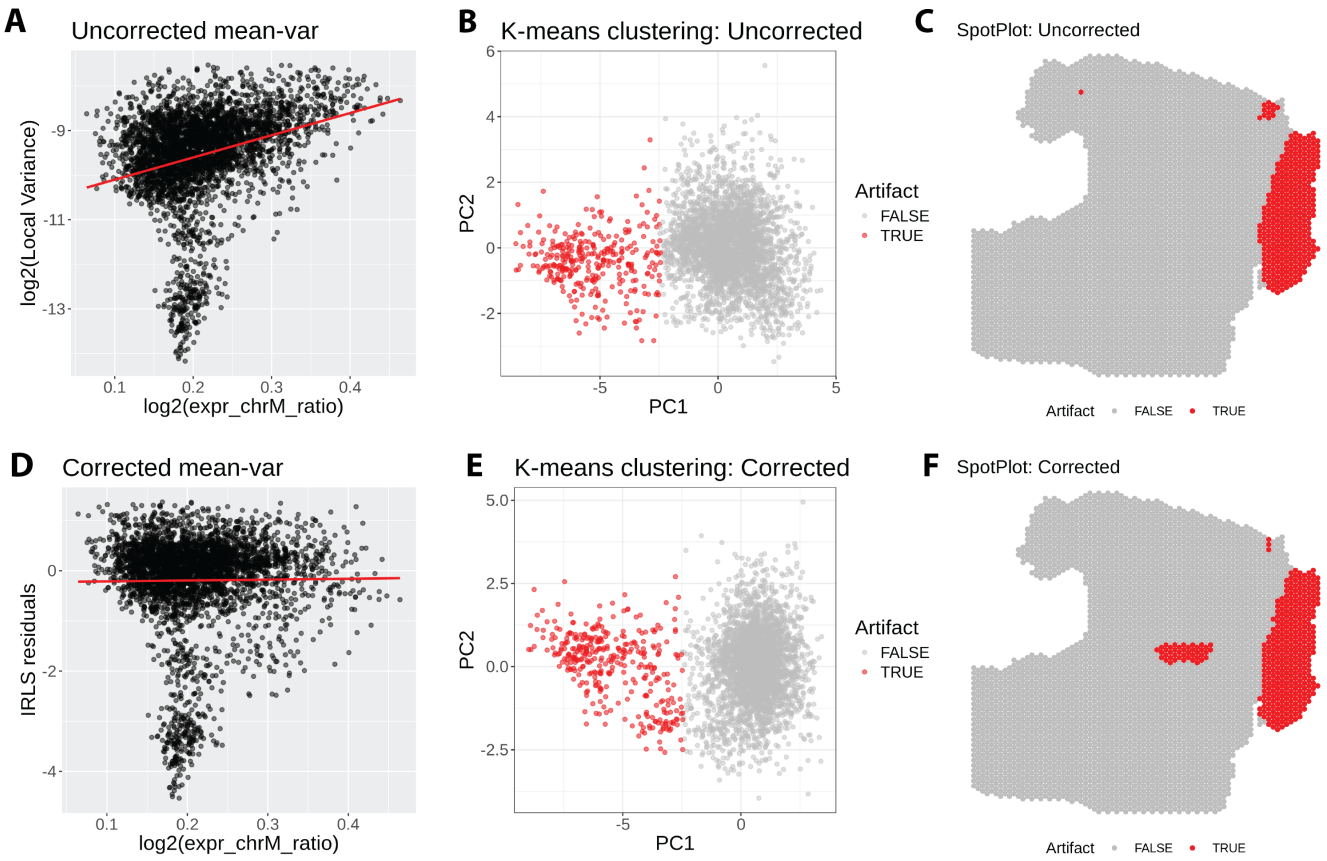

Supplementary Figure S8: Relationship between the mean and local variance of mitochondrial ratio. (A) Scatter plot showing that the local variance of mitochondrial ratio is positively associated with the local mean of mitochondrial ratio, both calculated at third-order neighbors. (B) Scatter plot of the Principle Components (PCs) 1 and 2 of the multiscale variances without accounting for the mean-variance relationship. Colored by k-mean clusters (k=2) of the predicted artifact (red) and the predicted un-compromised area (gray). (C) Spot plot showing the classification of k-means clusters without accounting for the relationship. (D) Scatter plot of the residuals versus mitochondria ratio when regressing the local variances (at 3rd-order neighbors) on the log2-transformed mitochondria ratio. (E) K-mean clustering (k=2) using the PCs 1 and 2 of the adjusted multiscale variance. (F) Spot plot showing the classification of k-means clusters using the adjusted data.

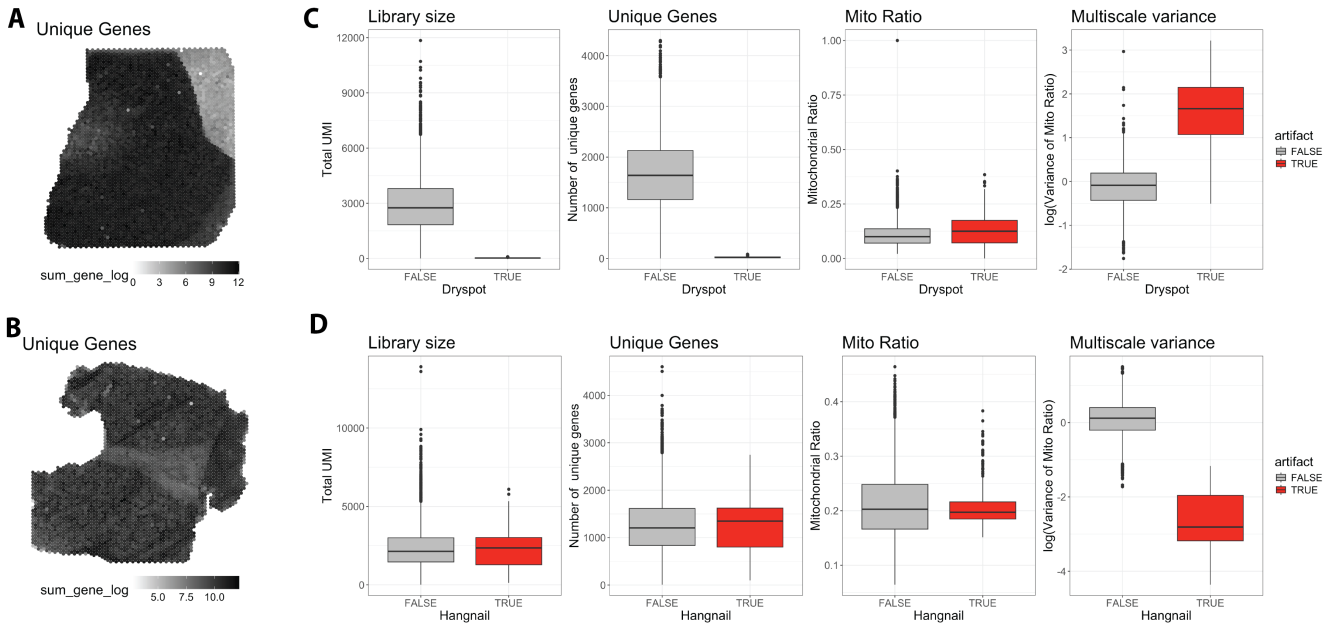

Supplementary Figure S9: Characterization of regional artifacts based on standard QC metrics and SpotSweeper's multiscale variance. Spot plots showing that the number of unique genes (log-transformed) in dryspot (A) and hangnail artifacts (B). (C) Box plots demonstrating that dryspot artifacts display lower library size and unique genes detected, but no difference in mitochondrial ratio. Dryspots do display higher multiscale variance (measured as the average of the local variances across scales) in mitochondrial ratio. (D) Box plots demonstrating that hangnail artifacts display no mean differences in library size, number of unique genes, or mitochondrial ratio. Hangnails do, however, display lower multiscale variance in the mitochondrial ratio. All box plots display the median with upper and lower quartiles, whiskers represent min and max. Black data points represent outliers.

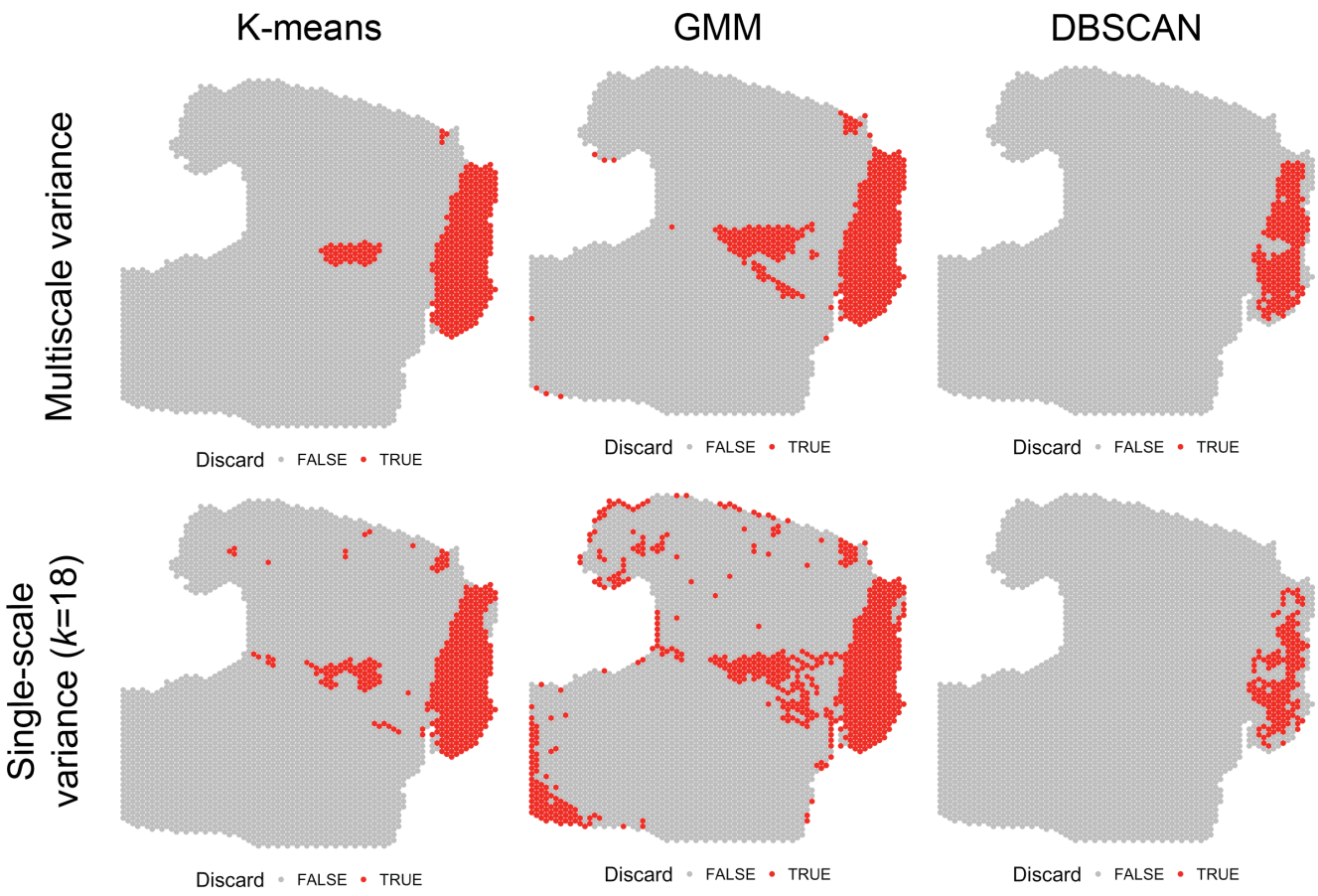

Supplementary Figure S10: Multiscale variances with k-means ($k = 2$) clustering shows the best performance in identifying regional artifacts. (Rows) Comparison of hangnail detection using multiscale variances (1-5 concentric circle per spot) versus single-scale ($k = 18$; one concentric circle per spot). (Columns) Clustering results to identify compromised regions using k-means ($k = 2$), Gaussian mixed models ($k = 2$), and DBSCAN methods.